

## STRONGLY NONLINEAR NATURE OF INTERFACIAL-SURFACTANT INSTABILITY OF COUETTE FLOW

Alexander L. Frenkel<sup>1</sup>, David Halpern<sup>2</sup>

<sup>1</sup> University of Alabama, Tuscaloosa, AL 35487-0350, USA  
email: afrenkel@gp.as.ua.edu

<sup>2</sup> University of Alabama, Tuscaloosa, AL 35487-0350, USA  
email: dhalpern@as.ua.edu

July 17, 2018

### Abstract

Nonlinear stages of the recently uncovered instability due to insoluble surfactant at the interface between two fluids are investigated for the case of a creeping plane Couette flow with one of the fluids a thin film and the other one a much thicker layer. Numerical simulation of strongly nonlinear longwave evolution equations which couple the film thickness and the surfactant concentration reveals that in contrast to all similar instabilities of surfactant-free flows, no amount of the interfacial shear rate can lead to a small-amplitude saturation of the instability. Thus, the flow is stable when the shear is zero, but with non-zero shear rates, no matter how small or large (while remaining below an upper limit set by the assumption of creeping flow), it will reach large deviations from the base values— of the order of the latter or larger. It is conjectured that the time this evolution takes grows to infinity as the interfacial shear approaches zero. It is verified that the absence of small-amplitude saturation is not a singularity of the zero surface diffusivity of the interfacial surfactant.

**AMS Subject Classification:** 76E17, 76E30

**Key Words and Phrases:** Two fluids; Couette; Insoluble surfactant; Nonlinear saturation of instability; Pattern formation

### 1. Introduction

Recently, a new instability of a channel flow of two fluid layers was uncovered in Frenkel & Halpern [1], Halpern & Frenkel [2]. This linear instability was further investigated in Blyth & Pozrikidis [3], Blyth & Pozrikidis [4], Wei [5], Frenkel & Halpern [6], Wei [7] (Blyth & Pozrikidis [3] and Blyth & Pozrikidis [4] included some nonlinear investigations). It is driven by the interaction of capillary and Marangoni forces with the interfacial shear of

the base flow, and does not depend on gravity and inertia for its realization. The instability disappears if the shear is zero. On the other hand, as was noted in Frenkel & Halpern [1], a nonzero shear is known to enable the nonlinear saturation of different instabilities, in which capillarity plays a stabilizing role and the destabilizing factor can be molecular Van der Waals forces (Babchin et al [8]), or gravity (Babchin et al [9], Halpern & Frenkel [10]), or the interfacial jump in viscosity (Hooper & Grimshaw [11], Shlang et al [12]), or capillary forces due to the azimuthal curvature of the interface in core-annular flows (Frenkel et al [13], Papageorgiou et al [14], Halpern & Grotberg [15]) (see also reviews Joseph & Renardy [16], Joseph et al [17]). When the shear rate is sufficiently large, the instabilities saturate with the final amplitude of the interface undulations being small, so that the whole evolution starting from small disturbances can be described by a weakly-nonlinear equation for the film thickness. (The mechanism of this nonlinear saturation was proposed in Babchin et al [9] and further clarified in Frenkel et al [13].) In other cases, the saturated amplitudes for certain regimes are large and a strongly nonlinear equation is appropriate, as for example for the flow down a fiber (Frenkel [18], Frenkel [19], Kerchman & Frenkel [20], Kalliadasis & Chang [21], Chang & Demekhin [22], Kliakhandler et al [23]) or for the core-annular flow (Frenkel & Kerchman [24], Kerchman [25], Joseph et al [17]). However, for the same systems, there are other parametric regimes for which small-amplitude saturation still occurs, so that the weakly-nonlinear description is good. Since for the instability considered below the interfacial shear of velocity plays two conflicting roles, working both for the linear instability and the nonlinear mechanism of saturation (and also because the dynamics involves a surfactant evolution equation in addition to the film thickness equation, in contrast to the single-equation description of evolution in the surfactant-free instabilities), there is a question whether there are any parametric domains for which the small-amplitude saturation of the interfacial-surfactant instability happens (Frenkel & Halpern [1]). In this paper, we investigate the nonlinear stages of the instability with respect to this question (and, to anticipate, arrive at the conclusion that no small-amplitude saturation occurs, so that the weakly-nonlinear description inevitably breaks down after some time).

The rest of the paper is organized as follows. In the next section, after giving the exact formulation of the Navier-Stokes problem, we use the lubrication approximation to obtain a simplified system of coupled equations for the film thickness and the surfactant concentration. The linear stability governed by these equations is studied in section 3 and the nonlinear evolution is numerically simulated in section 4. The last section contains the discussion of results and conclusions.

## 2. Problem formulation

### 2.1 Exact dynamic equations

The formulation of the exact Navier-Stokes problem (as given earlier in Frenkel & Halpern [1], Halpern & Frenkel [2]) is as follows. Consider two immiscible fluid layers between two infinite parallel plates, as in Fig. 1. Let the base flow be driven by the combined action of an in-plane steady motion of one of the plates and a constant pressure gradient parallel to the plate velocity and directed in either the same or the opposite sense. It is well known that the base “Couette-Poiseuille” velocity profiles are steady and vary (quadratically) in the spanwise direction only, and the base interface between the fluids is flat. For simplicity, let the densities of the two fluids be equal. Then gravity does not affect stability of the base flow, and is disregarded below. Let  $y^*$  be the spanwise, “vertical”, coordinate (the symbol  $*$  indicates a dimensional quantity). Let the interface be at  $y^* = d_1$  where  $d_1$  is the thickness

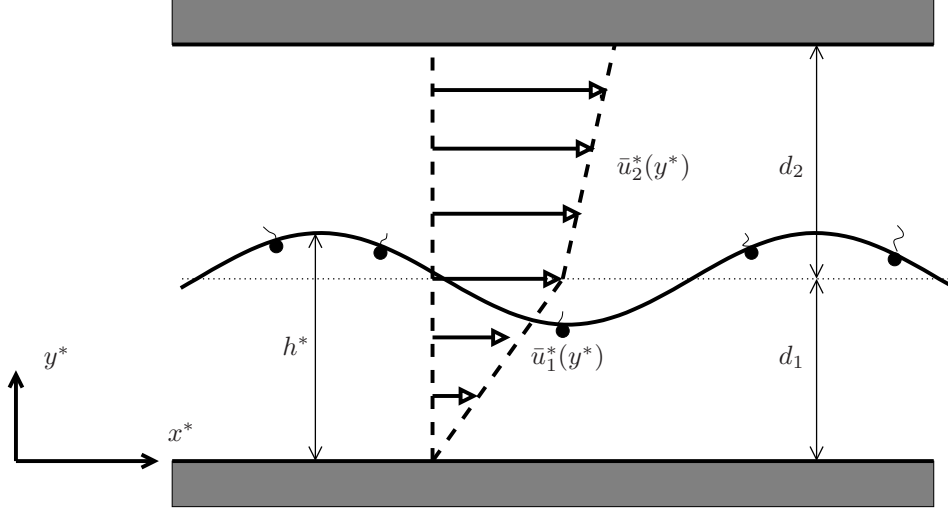


Figure 1: Definition sketch for a viscous two-layer Couette flow between a fixed plate at  $y^* = 0$  and a moving plate at  $y^* = d_1 + d_2$ . The disturbed interface  $y^* = h^*(x^*, t^*)$  is shown as a sinusoidal curve.  $\Gamma^*(x^*, t^*)$  is the concentration of the insoluble surfactant monolayer shown as discs with tails. The base velocity profiles are shown by bold arrows.

of the thinner layer, and the  $y^*$ -axis directed from the thinner layer (“film”) to the thicker one; we will call this the “upward” direction (clearly, since there is no gravity, the notions of “up” and “down” are a matter of convention). Thus,  $d_1 < d_2$  holds, where  $d_2$  is the thickness of the upper fluid. The direction of the “horizontal”  $x^*$ -axis is chosen so that velocity at the interface is positive, say  $U_1$  (whereas the velocity at the lower plate is zero).

The Squire-type theorem for the case with surfactants, proved in Halpern & Frenkel [2], allows us to confine the stability considerations to *two-dimensional* perturbed flows (in the  $x^*y^*$ -plane). The equation of the interface is  $y^* = h^*(x^*, t^*)$ , where  $h^*$  is the film thickness. The Navier-Stokes and incompressibility equations governing the fluid motion in the two layers are (with  $j = 1$  for the lower layer and  $j = 2$  for the upper one)

$$\rho \left( \frac{\partial \mathbf{v}_j^*}{\partial t^*} + \mathbf{v}_j^* \cdot \nabla^* \mathbf{v}_j^* \right) = -\nabla^* p_j^* + \mu_j \nabla^{*2} \mathbf{v}_j^*, \quad \nabla^* \cdot \mathbf{v}_j^* = 0$$

where  $\nabla^* = (\frac{\partial}{\partial x^*}, \frac{\partial}{\partial y^*})$ ,  $\rho$  is the density (of both fluids),  $\mathbf{v}_j^* = (u_j^*, v_j^*)$  is the fluid velocity with the horizontal component  $u_j^*$  and vertical component  $v_j^*$ , and  $p_j^*$  is the pressure.

We use the “no-slip, no-penetration” boundary conditions (requiring zero relative velocities) at the plates:  $u_1^* = 0, v_1^* = 0$  at  $y^* = 0$ ; and  $u_2^* = U_2, v_2^* = 0$  at  $y^* = d_1 + d_2$ , where  $U_2$  is the velocity of the upper plate (which can be positive or negative for the general Couette-Poiseuille flow). The interfacial boundary conditions are as follows. The velocity must be continuous at the interface:  $[\mathbf{v}^*]_1^2 = 0$ , where  $[A]_1^2 = A_2 - A_1$  denotes the jump in  $A$  across the interface, i.e. at  $y^* = h^*(x^*, t^*)$ . The interfacial balances of the tangential and normal stresses taking into account the jump in the tangential stress (due to the variability of surface

tension) as well as the capillary jump in the normal stress, at  $y^* = h^*(x^*, t^*)$ , are

$$\begin{aligned} \frac{1}{1+h_{x^*}^{*2}} [(1-h_{x^*}^{*2})\mu(u_{y^*}^*+v_{x^*}^*)+2h_{x^*}^{*2}\mu(v_{y^*}^*-u_{x^*}^*)]_1^2 &= -\frac{\sigma_{x^*}^*}{(1+h_{x^*}^{*2})^{1/2}} \\ [(1+h_{x^*}^{*2})p^*-2\mu(h_{x^*}^{*2}u_{x^*}^*-h_{x^*}^*(u_{y^*}^*+v_{x^*}^*)+v_{y^*}^*)]_1^2 &= \frac{h_{x^*}^{*2}}{(1+h_{x^*}^{*2})^{1/2}}\sigma^* \end{aligned}$$

where  $\sigma^*$  is the surface tension (the subscripts  $x^*, y^*, t^*$  denote the corresponding differentiation). The kinematic boundary condition (the conservation of mass condition) is

$$\frac{\partial h^*}{\partial t^*} + \frac{\partial}{\partial x^*} \int_0^{h^*(x^*, t^*)} u^* dy^* = 0. \quad (1)$$

The surface concentration of the insoluble surfactant on the interface,  $\Gamma^*(x^*, t^*)$ , obeys the following equation (see a simple derivation in Halpern & Frenkel [2]):

$$\frac{\partial(H\Gamma^*)}{\partial t^*} + \frac{\partial}{\partial x^*} (H\Gamma^*u^*) = D_s \frac{\partial}{\partial x^*} \left( \frac{1}{H} \frac{\partial \Gamma^*}{\partial x^*} \right) \quad (2)$$

where  $H = \sqrt{1+h_{x^*}^{*2}}$ , and  $D_s$  is the surface molecular diffusivity of surfactant;  $D_s$  is usually negligible, and is discarded below. We assume that the surfactant concentration  $\Gamma^*(x^*, t^*)$  is sufficiently small, remaining always far below its saturation value, so that the linear dependence of the surface tension on the surfactant concentration is a good approximation (see Edwards et al [26], p. 171):  $\sigma^* = \sigma_0 - E(\Gamma^* - \Gamma_0)$ , where  $\Gamma_0$  is the base surfactant concentration,  $\sigma_0$  is the base surface tension and  $E$  is a constant.

We use the following nondimensionalization:

$$(x, y) = \frac{(x^*, y^*)}{d_1}, \quad t = \frac{t^*}{d_1\mu_1/\sigma_0}, \quad (u, v) = \frac{(u^*, v^*)}{\sigma_0/\mu_1}, \quad p = \frac{p^*}{\sigma_0/d_1}, \quad \Gamma = \frac{\Gamma^*}{\Gamma_0}, \quad \sigma = \frac{\sigma^*}{\sigma_0}. \quad (3)$$

In the base flow, the interface is flat,  $\bar{h} = 1$ , and the surfactant concentration is uniform,  $\bar{\Gamma} = 1$ , where the overbar indicates a base-state quantity. Since the base flow has a constant pressure gradient, say  $2q$ , the two layers have equal pressures,  $\bar{p}_1 = \bar{p}_2 = 2qx$ , and the velocity profiles are

$$\bar{u}_1(y) = ry + qy^2, \quad \bar{v}_1 = 0, \quad \text{for } 0 \leq y \leq 1, \quad (4)$$

$$\bar{u}_2(y) = (r+q)\frac{m-1}{m} + \frac{r}{m}y + \frac{q}{m}y^2, \quad \bar{v}_2 = 0, \quad \text{for } 1 \leq y \leq n+1, \quad (5)$$

where  $n = d_2/d_1$  is the aspect ratio,  $n \geq 1$ , and  $m = \mu_2/\mu_1$ . The pair of constants  $r$  and  $q$  is used in place of the physical control parameters, the relative velocity of the plates and the pressure gradient, to characterize the base flow. The base interfacial velocity is  $w = r+q$ , so  $r+q > 0$ . The parameter  $s = r+2q$  is the interfacial shear of velocity (on the lower-fluid side).

## 2.2 Longwave (lubrication) approximation

We will assume that the aspect ratio is large,  $n \gg 1$  (actually we work in the zeroth order of the small parameter  $1/n$ , so the parameter  $n$  disappears from the equations). For sufficiently slow flow, the inertia terms in the Navier-Stokes equations are negligible. In the well-known lubrication approximation, which implies that the streamwise characteristic lengthscale is

much larger than the film thickness (see, e.g., the review papers Frenkel & Indireskumar [27] and Oron et al [28]), the simplified dynamic equations are, in the dimensionless form,

$$\frac{\partial p}{\partial x} = \frac{\partial^2 u}{\partial y^2}, \quad (6)$$

$$\frac{\partial p}{\partial y} = 0, \quad (7)$$

$$\frac{\partial v}{\partial y} = -\frac{\partial u}{\partial x}, \quad (8)$$

where  $u = u_1 - \bar{u}_1$ ,  $v = v_1 - \bar{v}_1$ , and  $p = p_1 - \bar{p}_1$ .

The no-slip no-penetration boundary conditions at the lower plate prescribe that

$$u = 0 = v \quad \text{at} \quad y = 0.$$

As usual for this class of systems with infinitely large aspect ratio (e.g., Babchin et al [8], Babchin et al [9], Hooper [29], Frenkel et al [13]), the disturbance quantities of the thick layer are negligible in the interfacial stress boundary conditions (at least if the viscosity ratio is not too different from one, so that at  $y = h(x, t)$  the difference of base velocities is not much larger than  $u$ , and hence  $u$  and the corresponding velocity disturbance in the thick layer are of the same order of magnitude), so the simplified boundary conditions at  $y = h(x, t)$  for the system (6-8) are

$$p = -[1 - M(\Gamma - 1)]h_{xx}$$

(the curvature term is retained to allow for the possibility of large surface values of tension) and

$$u_y = -M\Gamma_x$$

where the Marangoni number  $M$  is defined as  $M = E\Gamma_0/\sigma_0$ , and we have neglected  $h_x^2$  (as compared to 1) as well as some other terms, in accordance with the longwave (small-slope) approximation. The solution for  $u$  in terms of  $h(x, t)$  and  $\Gamma(x, t)$  is

$$u = \{h[(1 + M - M\Gamma)h_{xx}]_x - M\Gamma_x\}y - \frac{1}{2}[(1 + M - M\Gamma)h_{xx}]_x y^2.$$

We substitute the total velocity  $u_1 = ry + qy^2 + u$  into (i) the dimensionless mass conservation equation (1),  $h_t + \left[ \int_0^{h(x,t)} u_1(x, y, t) dy \right]_x = 0$ , and (ii) the simplified surfactant conservation equation

$$\Gamma_t + [\Gamma(rh + qh^2 + u)]_x = 0$$

(with  $u$  being evaluated at the interface  $y = h(x, t)$ ), where we have set  $H = 1$  (since  $h_x^2 \ll 1$ ) and the right-hand side of equation (2) to zero since the molecular diffusivity  $D_s$  is usually very small. As a result, we obtain a system of two coupled evolution equations, for  $h$  and  $\Gamma$ :

$$h_t + \left( r \frac{h^2}{2} + q \frac{h^3}{3} - M\Gamma_x \frac{h^2}{2} + \frac{1}{3}[(1 + M - M\Gamma)h_{xx}]_x h^3 \right)_x = 0, \quad (9)$$

$$\Gamma_t + \left[ \Gamma \left( rh + qh^2 - M\Gamma_x h + \frac{1}{2}h^2[(1 + M - M\Gamma)h_{xx}]_x \right) \right]_x = 0. \quad (10)$$

The terms containing  $r$  and  $q$  are clearly due to the nonzero base velocity.

To simplify, we make some additional assumptions: We assume  $q = 0$  (then the velocity is piecewise-linear and  $r$  is its slope in the film; also  $r$  is equal to the interfacial velocity) and  $M \ll 1$ , and also  $M\Gamma \ll 1$ . Rescaling  $\tilde{x} = \beta x$  and  $\tilde{t} = r\beta t$  where  $\beta = (3M/2)^{1/2}$ , introducing the constant  $C = \beta M/2r = (3M^3/(8r^2))^{1/2}$ , and dropping the tildes from the new variables, the equations take the form

$$h_t + \left[ \frac{h^2}{2} + C(-\Gamma_x h^2 + h_{xxx} h^3) \right]_x = 0, \quad (11)$$

$$\Gamma_t + \left[ \Gamma \left( h + C(-2\Gamma_x h + \frac{3}{2} h^2 h_{xxx}) \right) \right]_x = 0. \quad (12)$$

In each of these equations, the second term is due to the interfacial shear, the third one is due to Marangoni forces, and the last one describes the effect of capillarity.

In the rescaled variables, the longwave requirement reads

$$|\beta h_x| \ll 1$$

which, assuming  $M^{1/2} \ll 1$ , can be satisfied even in some cases with  $h_x \gtrsim 1$  (note that the unit of length for  $x$  is much greater than that for  $h$ ).

Note that because of the conservative form of the equations (11) and (12), the integral quantities  $\int h(x, t) dx$  and  $\int \Gamma(x, t) dx$  are time-independent if they are taken over domains with periodic boundary conditions.

We note that it is not difficult to obtain weakly-nonlinear evolution equations for the disturbances  $\eta$  and  $g$  defined by

$$h = 1 + \eta, \quad \Gamma = 1 + g.$$

One assumes the disturbances to be finite but small,

$$\eta \ll 1, \quad g \ll 1,$$

and retains only the leading-order linear and nonlinear terms in  $\eta$  and  $g$  in equations (11) and (12). Changing to the coordinate  $z = x - t$  (which eliminates the term  $\eta_x$  from equation (11) and the term  $g_x$  from equation (12)), we obtain

$$\eta_t + \left( \frac{\eta^2}{2} - C g_z + C \eta_{zzz} \right)_z = 0, \quad (13)$$

$$g_t + \left( \eta g + \eta - 2C g_z + \frac{3C}{2} \eta_{zzz} \right)_z = 0. \quad (14)$$

(In this derivation, for example the term proportional to  $g_z \eta_z$  coming from the third term in Eq. (11) is smaller by a factor of  $\eta \ll 1$  than the term proportional to  $g_{zz}$  arising from the same term in Eq. (11). Therefore, the smaller term has been dropped, while, on the other hand, the term with  $(\eta^2)_z$  has been retained in Eq. (13) as the leading order nonlinear term since there is no other term which would be clearly larger than it: Indeed, depending on the given conditions, the parameter  $C$  can take values ranging from very small to very large, and the same is true of the characteristic length scale measured in the units we have chosen. The only restriction on  $C$  is imposed by the requirement of smallness for the modified Reynolds number,  $Red_1/\Lambda \ll 1$ , where  $Re$  is the Reynolds number based on the interfacial velocity and the thickness  $d_1$ , and  $\Lambda/d_1$  is the dimensionless streamwise length scale of solutions.

This gives the constraint  $C \gg M^{3/2} \rho \sigma_0 d_1^2 / (\mu_1^2 \Lambda)$ . The nonlinear term in Eq. (14) is clearly smaller than the linear term  $\eta_z$  in view of  $g \ll 1$ ; it could be omitted and has only been retained in order to show the leading nonlinear term.)

These weakly-nonlinear evolution equations can be rescaled to a “canonical form” having just one parametric coefficient:

$$\eta_t + \eta \eta_z - g_{zz} + \eta_{zzzz} = 0, \quad (15)$$

$$g_t - g_{zz} + \frac{3}{4} \eta_{zzzz} + A \eta_z = 0 \quad (16)$$

(where the parameter  $A$  is inversely proportional to the parameter  $C$ ). [We notice that these weakly-nonlinear equations have certain similarities with the model system constructed for specific purposes in Malomed et al [30]: Both systems are first order in time and fourth order in space and have similar nonlinear terms, although couplings are different. For a review of other systems of coupled evolution equations, see, e.g., Glasman et al [31].] However, the above weakly-nonlinear equations turn out to be good for just a short transient stage: as we will see below, the small-amplitude saturation does not take place and disturbances quickly grow beyond the scope of the weakly-nonlinear equations. To repeat, this absence of the small-amplitude saturation in the interfacial-surfactant instability, contrasting with the presence of such small-amplitude saturation in all previously known surfactant-free instabilities of two-fluid flows, is the main point of the present communication.

### 3. Normal modes of infinitesimal disturbances

To examine behavior of infinitesimal disturbances to the steady uniform flow with  $\Gamma = 1$  and  $h = 1$ , we substitute  $h = 1 + \eta$  and  $\Gamma = 1 + g$  into Eqs. (11)-(12), and neglect the nonlinear terms, obtaining the linear system

$$\eta_t + \eta_x - C g_{xx} + C \eta_{xxxx} = 0, \quad (17)$$

$$g_t + g_x + \eta_x - 2C g_{xx} + \frac{3}{2} C \eta_{xxxx} = 0. \quad (18)$$

It is known (Frenkel & Halpern [1], Halpern & Frenkel [2]) that the normal modes  $(\eta, g) \propto e^{i\alpha x} e^{\gamma t} e^{i\omega t}$  where  $\alpha$  is the wavenumber,  $\gamma(\alpha)$  is the growth rate, and  $\omega(\alpha)$  is the time frequency, are unstable—if and only if  $C < \infty$  (i.e., the shear velocity  $r \neq 0$ )—for “long” waves,  $0 < \alpha < \alpha_0$ , where  $\alpha_0$  is a marginal wavenumber. The longwave asymptotic dependence of the growth rate is  $\gamma \propto \alpha^{3/2}$  as  $\alpha \rightarrow 0$ . The normal modes decay if  $\alpha > \alpha_0$ , with  $\gamma \sim -\frac{1}{4}\alpha^2$  as  $\alpha \rightarrow \infty$ . (We note that the decay is weaker than  $\alpha^4$  despite the presence of the fourth-derivative terms in the linearized equations (17) and (18)). Typical dispersion curves, the growth rate versus wavenumber, are shown in Fig. 2. They have the maximum value  $\gamma_{max}$  at a certain wavenumber  $\alpha_{max}$  depending on the value of the equation parameter  $C$ . These dependences are shown in Fig. 3.

Multiplying Eq. (17) by  $\eta$  and (18) and integrating over the interval of spatial periodicity, and taking into account that  $\eta$  and  $g$  are out of phase by nearly  $\pi$  in unstable modes, shows that the fourth derivative (capillary) term is stabilizing in Eq. (17) but destabilizing in Eq. (18). Similarly, the Marangoni term, the one with  $g_{xx}$ , is stabilizing for  $g$  but destabilizing with regard to  $\eta$ .

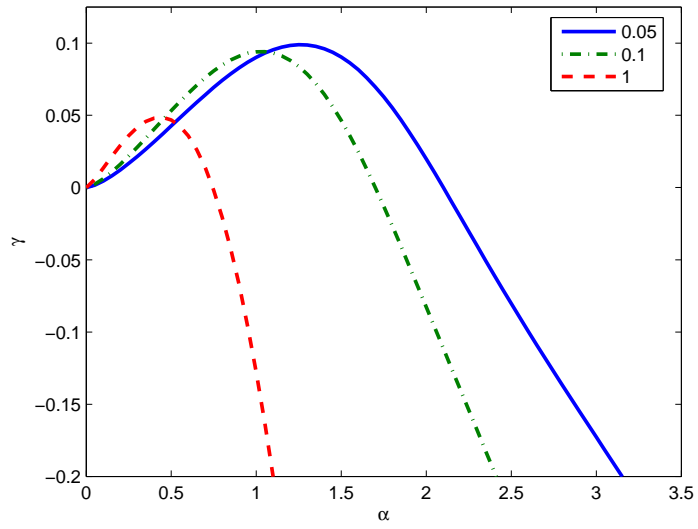


Figure 2: Dependence of the growth rate  $\gamma$  on the wavenumber  $\alpha$  of a normal mode for three values of the parameter  $C$  indicated in the legend.

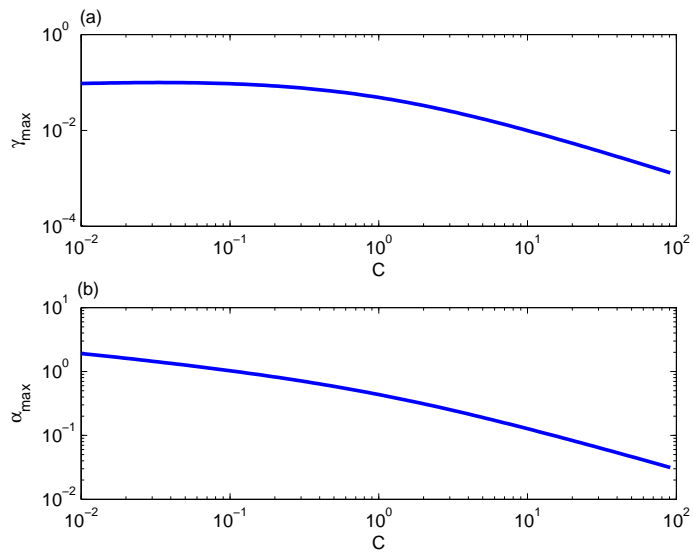


Figure 3: (a) Growth rate and (b) wavenumber of the fastest-growing normal mode versus  $C$ .



#### 4. Nonlinear numerical simulations

We solved the system of equations (11) and (12) numerically on  $0 \leq x \leq 2\pi Q$  with periodic boundary conditions using the method of lines. This involved the approximation of the spatial derivatives with finite differences and an implicit Gear's method for the time-stepping. The number of nodes in the spatial discretization ranged from hundreds to tens of thousands. Also, some results were checked using standard pseudospectral Fourier method (see e.g. Kerchman & Frenkel [20]) in conjunction with an implicit Gear's method for the time-stepping. The number of modes ranged from 256 to 1024 for different cases. We have used dealiasing as described e.g. in Kerchman & Frenkel [20] (similar to Canuto et al [32]), filtering out slightly more than three-fifths of the modes with higher wavenumbers from the unknown functions and their derivatives, computed in the Fourier space, before computing the nonlinear terms of the equations in the physical space. In all cases, we took care that the length of the interval determined by the parameter  $Q$  was sufficiently large to accommodate five or more elementary pulses, as it is known, e.g. for the Kuramoto-Sivashinsky equation, that the results can be sensitive to the type of boundary conditions and the length of the interval when the latter is not sufficiently large (Papageorgiou and Smyrlis [33], Frenkel & Indireskumar [27], Wittenber & Holmes [34]). [In particular, the preliminary nonlinear saturation results found—although for very different parametric regimes—in Blyth & Pozrikidis [3], may not hold for sufficiently large domains. We have checked that such was indeed the case for our semi-infinite flow configuration: The small-amplitude saturation occurring for a narrow band of values of  $Q$  near criticality, such that the periodicity interval accommodated just one unstable normal mode, disappeared for larger values of  $Q$ , since the corresponding larger intervals can accommodate additional longwave modes which are unstable. Of course, to any one-pulse solution for a small  $Q = a$  there is a corresponding solution for an  $n$  times larger value,  $Q = na$ , consisting of  $n$  identical  $a$ -pulses. However, as a rule, this  $n$ -pulse solution is unstable to longwave disturbances and therefore is not observed as an outcome of evolution. Conversely, the results are essentially insensitive to further increase of  $Q$  chosen in this way.]

For the initial conditions we use small-amplitude white-noise deviations from the base uniform profiles. The deviation values at the spatial nodes are chosen from the uniform random number distribution on the interval  $[-10^{-2}, 10^{-2}]$ . Typical initial profiles are shown in Fig. 4.

In the subsequent evolution, the shortwave normal modes die out, but the longwave ones grow, and the spatial profiles evolve to the pulse trains, like the travelling waves shown in Fig. 5(a). A typical evolution of the instantaneous global maxima and minima of the spatial profiles of the surfactant concentration  $\Gamma$  and the film thickness  $h$  is shown in Fig. 5(bc): There, the deviations of  $\Gamma$  and  $h$  saturate but at levels which are not small as compared to non-disturbed values. In Fig. 6, the evolution for different parameter values is shown to emphasize the point that the deviations in all cases grow to levels of order one. To this end, each time series is followed up to the instant at which the minimum surfactant concentration reaches the representative level of 0.5. We used five different values of the equation parameter  $C$ , from small to order one to large:  $10^{-2}$ ,  $10^{-1}$ , 1, 10, and  $10^2$ , with sufficiently large values of  $Q$  (as discussed above; also, in all cases, we have checked that refining the spatial and temporal resolutions does not change the results.). The figure clearly shows that in all cases the deviations of the surfactant concentration and the film thickness grow and become non-small in comparison with their base values. As a result, the weakly nonlinear equations (15) and (16), based on the assumption that the deviations are small, would cease to be good. (Also, clearly, if the film thickness becomes sufficiently small as for  $C = 100$  (see Fig. 6(b)), the molecular van der Waals forces should be taken into account.) The greater the value of  $C$ , the larger time (of the governing equations) the evolution takes.

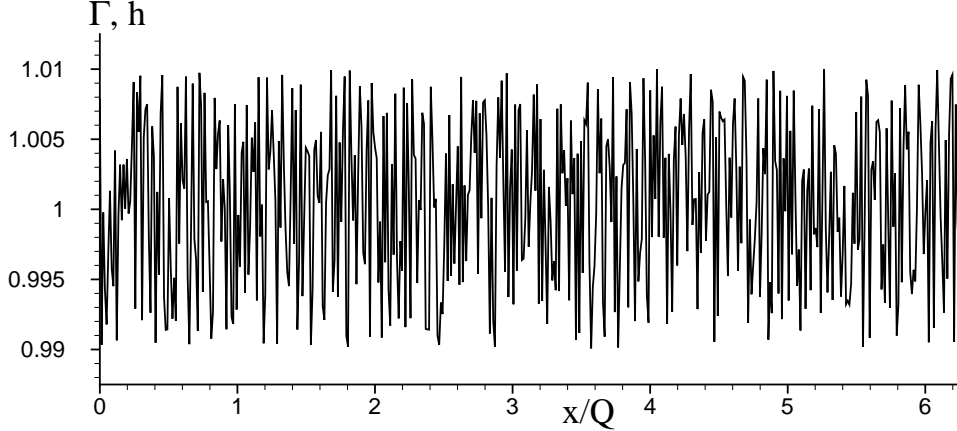


Figure 4: Typical initial profile of surfactant concentration or film thickness: a white noise distribution, with deviation amplitude of  $10^{-2}$  for 512 modes.

As was mentioned above, the initial configuration with many maxima and minima (see Fig. 4) quickly evolves, by coalescences, to just a few pulses (see Fig. 5a). Another way to describe this is to note that the normal modes with large wavenumbers are damped and die out. The normal mode of the fastest growth has a tendency to dominate, at least initially. We can define an effective wavenumber  $\alpha_{eff}$  of an instantaneous profile to be  $2\pi$  over the “length per one pulse”. The latter is the interval length  $2\pi Q$  divided by the number of pulses  $N$ . Therefore,  $\alpha_{eff} = N/Q$ . The dependence of  $\alpha_{eff}$  on  $C$  is shown in Fig. 7(a) together with that of the wavenumber  $\alpha_{max}$  of the fastest growing normal mode. These are seen to be close throughout the entire range of  $C$  shown in Fig. 7(a).

We also define an effective growth rate  $\gamma_{eff}$  to be that of a (hypothetical) normal mode that would have the same minimum surfactant concentration as the actual nonlinear profile at two instances of time,  $t = 0$  and  $t = t_1$ , where  $t_1$  is determined by  $\Gamma_{min}(t_1) = 0.5$ . This gives  $\gamma_{eff} = \log(0.5/10^{-2})/t_1$ , that is  $\gamma_{eff} = \log(50)/t_1$ . Fig. 7(b) shows  $\gamma_{eff}$  (inversely proportional to the evolution time  $t_1$ ) as a function of  $C$ . For comparison, the growth rate  $\gamma_{max}$  of the fastest growing normal mode is included in the figure.  $\gamma_{eff}$  is always smaller than  $\gamma_{max}$  because the initial exponential growth of small disturbances slows down as the magnitude of the disturbances grows. The figure also reflects on the fact that the evolution time grows with  $C$ . We conjecture that  $t_1 \rightarrow \infty$  as  $C \rightarrow \infty$ —that is, (assuming that  $M$  is fixed), as the shear rate approaches zero. (It is easy to see that this would mean that the corresponding physical, dimensional, time of the evolution diverges to infinity as well.)

The above results have been obtained discarding surfactant diffusion. To check the continuity in the surfactant diffusivity at its zero value, we should add into the left-hand side of equation (12) the term  $-D\Gamma_{xx}$ , where  $D$  is a constant proportional to  $D_s$ , the surface molecular diffusivity of surfactant. We have simulated the modified equations with the values of  $D$  as large as 0.1. The results turned out to be qualitatively the same as with  $D = 0$  (see Fig. 8).

## 5. Discussion and conclusions

We have investigated the nonlinear stages of the insoluble-surfactant instability in a sheared viscous film in a semi-infinite plane-Couette flow. Numerical simulations of strongly non-

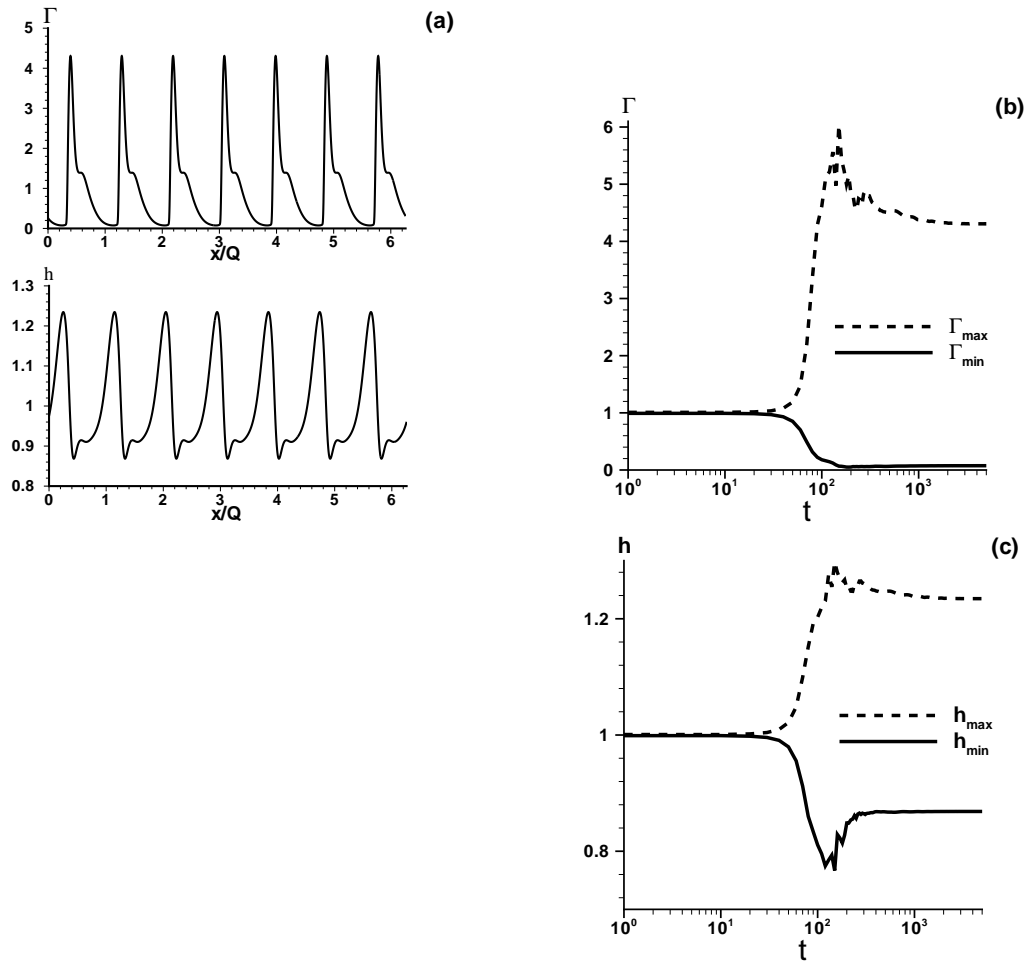


Figure 5: A typical evolution of the surfactant concentration and film thickness. (a) The saturated travelling-wave profiles of the surfactant concentration and the film thickness, at  $t = 5000$ . (b) The time dependence of the minimum and maximum (over  $x$ ) surfactant concentration. (c) The time dependence of the minimum and maximum film thickness. Here  $C = 10^{-2}$  (and  $Q = 5.2$ ).

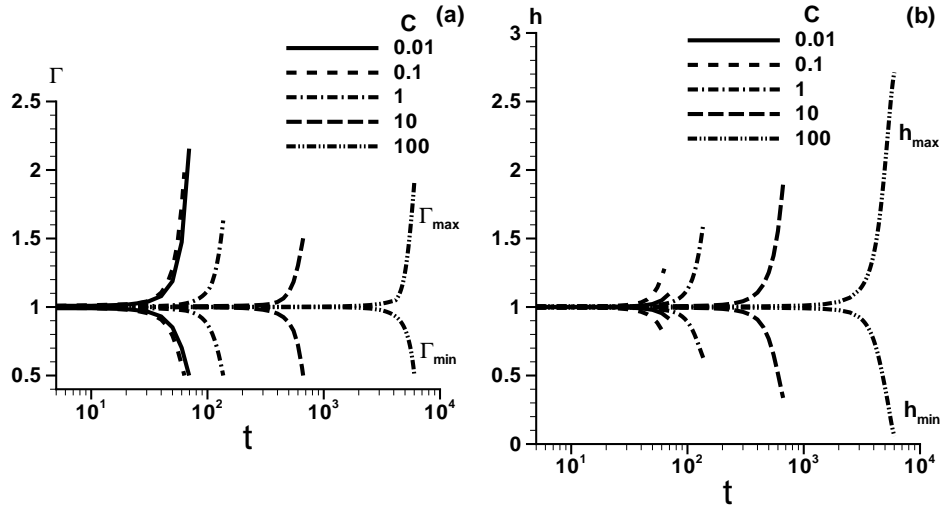


Figure 6: Evolution of (a) surfactant concentration and (b) film thickness: The dependence of the minimum and maximum (over  $x$ ) values  $\Gamma_{max}$ ,  $\Gamma_{min}$  and  $h_{max}$ ,  $h_{min}$  on time  $t$ , for the five different values of  $C$  shown in the legend. Each evolution is shown up to the time at which the minimum surfactant concentration reaches the value of 0.5. (In the order of increasing  $C$ , the values of  $Q$  used in these simulations are 5.2, 8, 18, 50, 250.)

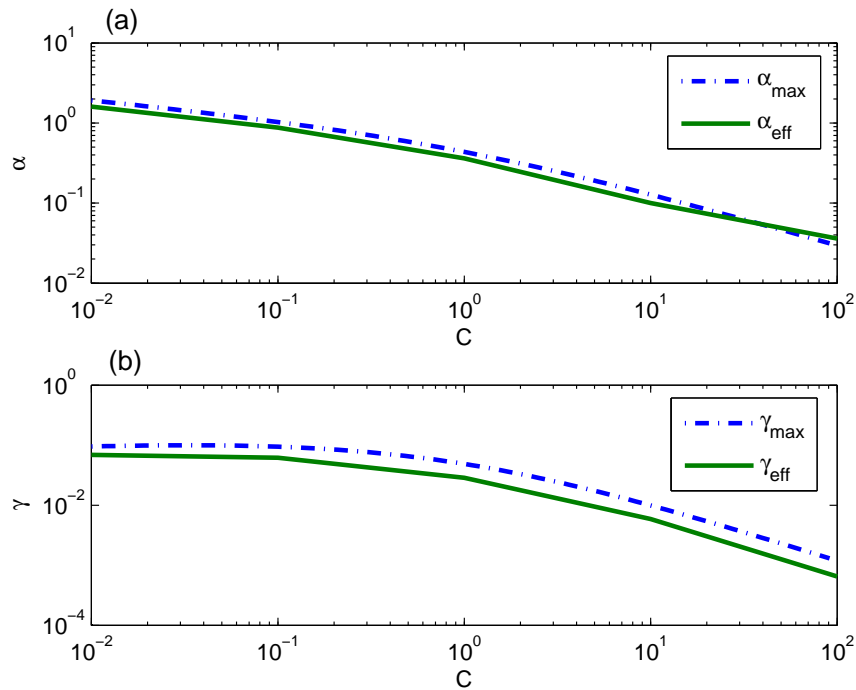


Figure 7:  $C$ -dependence of (a) the effective wavenumber and (b) the effective growth rate (defined in the text). For comparison the corresponding linear-theory quantities  $\gamma_{max}$  and  $\alpha_{max}$  are included.

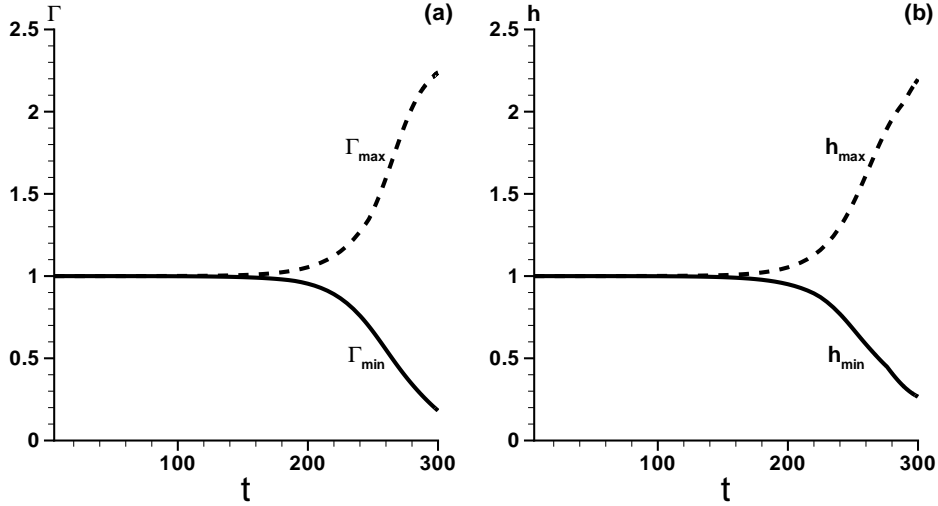


Figure 8: Same as Fig. 6 but for a non-zero diffusivity  $D$  value. Here  $D = 0.1$ ,  $C = 1$  ( $Q = 18$ ).

linear longwave evolution equations on extended spatial intervals show that the earlier uncovered remarkable property of the linear instability, the necessity of a non-zero interfacial shear rate for the system to be unstable to infinitesimal disturbances, has a “nonlinear continuation”: no matter how large or small the interfacial shear of the base flow, there is *no* small-amplitude saturation of the instability. (So the weakly non-linear equations cannot describe the large-time evolution.)

The impossibility of a small-amplitude saturation is corroborated by the following argument. Suppose there is such a saturated state of Eqs. (13) and (14) with  $N \ll 1$  and  $G \ll 1$ , where  $N$  and  $G$  are the saturated amplitudes of deviations of the film thickness and surfactant concentration, respectively, having the characteristic length scale  $L$  (such that  $\eta_z \sim N/L$  and  $g_z \sim G/L$ ) and time scale  $T$  (such that  $\eta_t \sim N/T$  and  $g_t \sim G/T$ ). Consider the dominant balance of terms in Eqs. (13) and (14). The only nonlinear term,  $\eta\eta_z$ , must be one of the dominant terms in Eq. (13). But at least one of the terms  $Cg_{zz}$  and  $C\eta_{zzzz}$  must be among the dominant terms there, since the dominant equation cannot be just  $\eta_t + \eta\eta_z = 0$ : this equation is well-known to lead to infinite slopes in finite time. Thus,  $N^2/L \sim \max(CG/L^2, CN/L^4)$ . But the same terms,  $Cg_{zz}$  and  $C\eta_{zzzz}$ , cannot be among the dominant ones in Eq. (14), since the term  $\eta_z$  there is much larger:  $N/L \gg N^2/L$ . Thus the dominant balance in Eq. (14) would have to be just  $g_t + \eta_z = 0$ , leading to  $\eta_z \sim g_t$ . Combining this relation with  $\eta_t \lesssim \eta\eta_z$  (see Eq. (13)), we can write  $\eta_t \lesssim \eta g_t \sim NG/T \ll N/T \sim \eta_t$ . Thus, we have arrived at  $\eta_t \ll \eta_t$ , a contradiction. Therefore, there can be no saturated solutions of the weakly-nonlinear equations (13)-(14) with both  $\eta$  and  $g$  being small; in other words, there can be no small-amplitude saturation of the instability in question. (This argument assumes a single time scale, which is generically the case. Only for a limited domain of near-critical states multiple time scales occur due to the presence of the small super-criticality parameter. As was mentioned above, under such non generic conditions the small-amplitude saturation does occur. This should be possible be describable by Landau type theory, which we plan to investigate in the future.)

The same considerations hold for the weakly nonlinear equations obtainable directly from

Eqs. (9-10). They imply that, even when the Marangoni number  $M$  is not small, the small-amplitude saturation of the interfacial-surfactant instability is impossible as well.

Our numerics show that when one includes into consideration (small) non-zero diffusion of the surfactant, the instability still does not saturate with small amplitudes, and the disturbances of the film thickness or/and the surfactant concentration reach values of order one. Evidently, the increase of the base shear does *not* lead to the small-amplitude saturation—as it does in all previously known similar systems without surfactants (which are described by a single evolution equation, the one for the film thickness). Thus, for the interfacial surfactant instability under consideration here, the increase of the saturating effect with the shear rate cannot overcome the simultaneous increase in the strength of the instability.

It remains to be seen if there is a threshold in the strength of the surfactant diffusivity above which a small-amplitude saturation of the instability will set in. We hope to fully investigate the effect of diffusion (including the questions of saturation, with small as well as with large amplitudes) in the future. Even without diffusion, the large-amplitude saturation is possible; an example is shown in Fig 5. The systematic investigation of the large-amplitude evolution, which is beyond the scope of this paper, will be a subject of the future study as well.

## References

- [1] A. L. Frenkel and D. Halpern. Stokes-flow instability due to interfacial surfactant. *Phys. Fluids*, 14(7):L45–L48, 2002.
- [2] D. Halpern and A. L. Frenkel. Destabilization of a creeping flow by interfacial surfactant: Linear theory extended to all wavenumbers. *J. Fluid Mech.*, 485:191–220, 2003.
- [3] M. G. Blyth and C. Pozrikidis. Effect of surfactants on the stability of two-layer channel flow. *J. Fluid Mech.*, 505:59–86, 2004.
- [4] M. G. Blyth and C. Pozrikidis. Effect of inertia on the Marangoni instability of two-layer channel flow, Part II: normal-mode analysis. *J. Engng Math.*, 50(2-3):329–341, 2004.
- [5] H. H. Wei. Effect of surfactant on the long-wave instability of a shear-imposed liquid flow down an inclined plane. *Phys. Fluids*, 17(1):012103, 2005.
- [6] A. L. Frenkel and D. Halpern. Effect of inertia on the insoluble-surfactant instability of a shear flow. *Phys. Rev. E*, 71(1):016302, 2005.
- [7] H. H. Wei. On the flow-induced Marangoni instability due to the presence of surfactant. *J. Fluid Mech.*, 544:173–200, December 2005.
- [8] A. J. Babchin, A. L. Frenkel, B. G. Levich, and G. I. Sivashinsky. Flow-induced nonlinear effects in thin liquid film stability. *Ann. NY Acad. Sci.*, 404:426–428, 1983.
- [9] A. J. Babchin, A. L. Frenkel, B. G. Levich, and G. I. Sivashinsky. Nonlinear saturation of Rayleigh-Taylor instability in thin films. *Phys. Fluids*, 26:3159–3161, 1983.
- [10] D. Halpern and A. L. Frenkel. Saturated Rayleigh-Taylor instability of an oscillating Couette film flow. *J. Fluid Mech.*, 446:67–93, 2001.

- [11] A. P. Hooper and R. Grimshaw. Nonlinear instability at the interface between two viscous fluids. *Phys. Fluids*, 28:37–45, 1985.
- [12] T. Shlang, G.I. Sivashinsky, A. J. Babchin, and Frenkel A. L. Irregular wavy flow due to viscous stratification. *Journal de Physique*, 46:863–866, 1985.
- [13] A. L. Frenkel, A. J. Babchin, B. G. Levich, T. Shlang, and G. I. Sivashinsky. Annular flow can keep unstable flow from breakup: nonlinear saturation of capillary instability. *J. Colloid Interface Sci.*, 115:225–233, 1987.
- [14] D.T. Papageorgiou, C. Maldarelli, and D.S. Rumschitzki. Nonlinear interfacial stability of core annular film flows. *Phys. Fluids A*, 2:268–271, 1990.
- [15] D. Halpern and J. B. Grotberg. Nonlinear saturation of the Rayleigh instability due to oscillatory flow in a liquid-lined tube. *J. Fluid Mech.*, 492:251–270, 2003.
- [16] D. D. Joseph and Y. Renardy. *Fundamentals of Two-Fluid Dynamics, vol I: Mathematical Theory and Applications*. Springer, 1993.
- [17] D. D. Joseph, R. Bai, K. P. Chen, and Y. Y. Renardy. Core-annular flows. *Ann. Rev. Fluid Mech.*, 29:65–90, 1997.
- [18] A. L. Frenkel. Nonlinear theory of strongly undulating thin films flowing down vertical cylinders. *Europhysics Letters*, 18(7):583–588, 1992.
- [19] A. L. Frenkel. On evolution equations for thin films flowing down solid surfaces. *Phys. Fluids A*, 5(10):2342–2347, 1993.
- [20] V. I. Kerchman and A. L. Frenkel. Interactions of coherent structures in a film flow - simulations of a highly nonlinear evolution equation. *Theor. Comp. Fluid Dyn.*, 6:235–254, 1994.
- [21] S. Kalliadasis and H. C. Chang. Drop formation during coating of vertical fibers. *J. Fluid Mech.*, 261:135–168, 1994.
- [22] H. C. Chang and E. A. Demekhin. Mechanism for drop formation on a coated vertical fibre. *J. Fluid Mech.*, 380:233–255, 1999.
- [23] I. L. Kliakhandler, S. H. Davis, and S. G. Bankoff. Viscous beads on vertical fibre. *J. Fluid Mech.*, 429:381–390, 2001.
- [24] A. L. Frenkel and V. I. Kerchman. On large amplitude waves in core-annular flows. In W. F. Ames, editor, *Proc. 14th IMACS Congress on Computations and Applied Mathematics*, volume 2, pages 397–400, Atlanta, GA, 1994.
- [25] V. Kerchman. Strongly nonlinear interfacial dynamics in core-annular flows. *J. Fluid Mech.*, 290:131–166, 1995.
- [26] D.A. Edwards, H. Brenner, and D.T. Wasan. *Interfacial transport processes and rheology*. Butterworth-Heinemann, Boston, 1991.
- [27] A. L. Frenkel and K. Indireskumar. Derivation and simulations of evolution equations of wavy film flows. In D. N. Riahi, editor, *Math Modeling and Simulation in Hydrodynamic Stability*, pages 35–81. World Scientific, Singapore, 1996.
- [28] A. Oron, S. H. Davis, and S. G. Bankoff. Long-scale evolution of thin liquid films. *Reviews of Modern Physics*, 69:931–980, 1997.

- [29] A. P. Hooper. Long-wave instability at the interface between two viscous fluids: Thin layer effects. *Phys. Fluids*, 28:1613–1618, 1985.
- [30] B. A. Malomed, B. F. Feng, and T. Kawahara. Stabilized Kuramoto-Sivashinsky system. *Phys. Rev. E*, 6404(4):046304, 2001.
- [31] E. A. Glasman, A. A. Golovin, and A. A. Nepomnyashchy. Instabilities of wavy patterns governed by coupled Burgers equations. *SIAM J. Appl. Math.*, 65(1):230–251, 2004.
- [32] C. Canuto, M. Y. Hussaini, A. Quarteroni, and T. A. Zang. *Spectral Methods in Fluid Dynamics*. Springer Verlag, New York, 1987.
- [33] D. T. Papageorgiou and Y. S. Smyrlis. The route to chaos for the Kuramoto-Sivashinsky equation. *Theoret. Comput. Fluid Dynamics*, 3:15–42, 1991.
- [34] R. Wittenber and P. Holmes. Scale and space localization in the Kuramoto-Sivashinsky equation. *Chaos*, 9:452–465, 1999.